Theoretical study of dislocation nucleation from simple surface defects in semiconductors

J. Godet,* L. Pizzagalli, S. Brochard, and P. Beauchamp
Laboratoire de Métallurgie Physique, CNRS UMR 6630, Université de Poitiers, B.P. 30179, 86962 Futuroscope Chasseneuil Cedex, France
(Received 16 April 2004; published 30 August 2004)

Large-scale atomistic calculations, using empirical potentials for modeling semiconductors, have been performed on a stressed system with linear surface defects like steps. Although the elastic limits of systems with surface defects remain close to the theoretical strength, the results show that these defects weaken the atomic structure, initializing plastic deformations, in particular dislocations. The character of the dislocation nucleated can be predicted considering both the resolved shear stress related to the applied stress orientation and the Peierls stress. At low temperature, only glide events in the shuffle set planes are observed. Then they progressively disappear and are replaced by amorphization/melting zones at a temperature higher than 900 K.

DOI: 10.1103/PhysRevB.70.054109 PACS number(s): 61.72.Lk, 61.72.Cc, 07.05.Tp, 02.70.Ns

I. INTRODUCTION

The plasticity of semiconductors has been a subject of numerous studies for the last decades in both fundamental and applied research. Despite significant progress in the understanding of the fundamental mechanisms involved, several issues remain, in particular for nanostructured semiconductors. In these materials, including for example nanograined systems or nano-layers in heteroepitaxy, dimensions are usually too small to allow the classical mechanisms of dislocation multiplication, such as Franck-Read sources.[1] It is then likely that other mechanisms dominate, and it has already been proposed that surfaces and interfaces, which become prominent for small dimensions, play a major role. Several observations support this assumption, especially for strained layers and misfit dislocations at interfaces.[2–4] The question of dislocation formation at surfaces also concerns bulk materials submitted to large stresses.[5–9] The propagation of dislocation from surfaces has been investigated in the frame of a continuum model and elasticity theory.[10–13] However, the characterization of the nucleation of dislocations is incomplete with this approach, and the predicted activation energy is very large, in disagreement with experiments. It is also difficult to investigate experimentally the very first stages of dislocation formation. In short, the mechanisms involved in the nucleation of dislocations from surfaces or interfaces are far to be well understood. There have been some attempts to perform atomistic calculations for addressing this issue. In particular, the interaction between a dislocation and the free surface or the interface,[14,15] or between ledges and a crack tip,[16] and the instability of a stressed ledge[17] have been studied.

It has been proposed that surface defects like steps, or cleavage ledges, could favor the nucleation of dislocations, by lowering the activation energy.[18] This assumption is supported by experimental facts, with dislocation sources located on the cleavage surface and coinciding with cleavage ledges.[19–22] Also partial dislocations can be formed from the surface during microindentation.[23] Atomistic simulations of dislocation nucleation from surface defects in metals have also been recently reported.[24] It has been shown that the presence of the step modifies the otherwise uniform strain field,[25] which effectively makes easier the dislocation formation. The situation appears to be different for semiconductors, with no clear strain inhomogeneity at the step.[26,27] The role of the stress orientation on the dislocation formation is also unclear. Additional atomistic simulations are needed to shed light on these points and fully characterize the mechanisms behind dislocation nucleation.

In this paper, we report large-scale atomistic calculations of the nucleation of dislocations from surface defects in systems submitted to a stress with variable orientation. We focused on linear surface defects like simple steps, but also cleavage ledges. As for the material, silicon was selected as the best candidate, for several reasons. First, it is a good model, since a lot of semiconductors crystallize in the same cubic diamond structure, or the zinc-blende structure, almost equivalent from the point of view of plasticity. Second, silicon can be grown without native dislocations, which allows a comparison between experiments and simulations. Finally, several high quality atomistic potentials are available. In the first part of the paper, the silicon structure and the slip systems are briefly described. After the presentation of the model and the calculations techniques used to perform the simulations, the results obtained with several empirical potentials are described. In particular, we mostly focus on stress orientations that increase the probability of nucleating the relevant dislocations. Several points are then discussed, such as the conditions for nucleation, the role of stress orientation and temperature, and the selected slip system.

II. METHODOLOGY

A. Structure and geometry

In ambient conditions, the stable structure of silicon is diamond cubic. Dislocations glide in the (111) dense planes, that are gathered together in two sets, one widely spaced, called the "shuffle" set and one narrowly spaced, called the "glide" set [Fig. 1(a)]. The Burgers vector of a perfect dislocation is $1/2\langle 1\bar{1}0\rangle$. Dissociation into two Shockley partial dislocations, $1/6\langle 1\bar{2}1\rangle$ and $1/6\langle \bar{2}11\rangle$ is possible through the formation of a stable stacking fault in the glide set.[28] Note

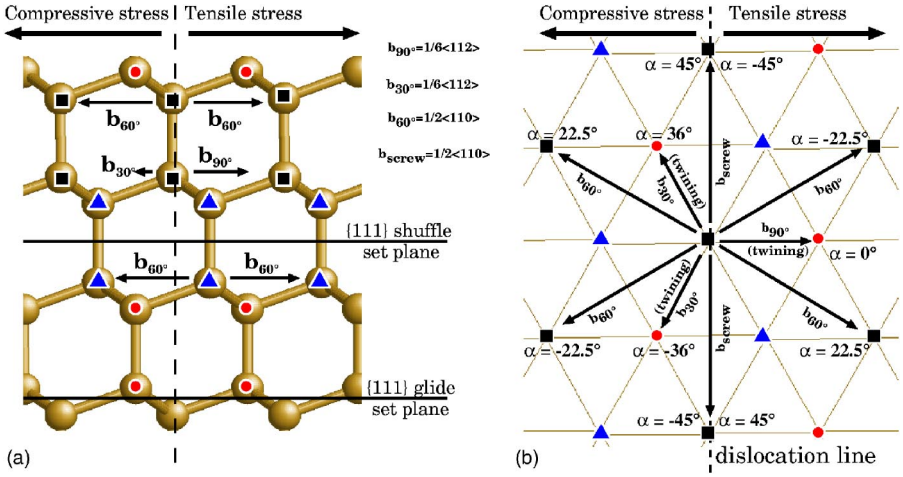

FIG. 1. Diamond-like structure projected along $[0\bar{1}1]$ (a) and along [111] (b). All the possible slip directions following the Burgers vectors of the 60°, 90°, 30° and screw dislocations are considered. For each dislocation, the best stress orientation giving the maximum resolved shear stress is indicated through angle α (see also Fig. 3).

that, since the Burgers vector of a partial dislocation does not link two points of the crystal lattice, the nucleation of a partial dislocation is always accompanied by a stacking fault in the glide set plane. When occurring on adjacent atomic planes, the stacking faults form micro-twins. Considering the angle between the dislocation line and the Burgers vector, perfect dislocations are called 60° or screw, while partials are called 90° or 30°. These notations are used in the rest of the paper.

A semi-infinite system including surface steps is modeled by a slab with a 2×1 reconstructed (100) free surface (Fig. 2).[29,30] Four atomic layers are frozen in the bottom of the slab, opposite to the free surface. Steps, lying along the $[0\bar{1}1]$ dense directions, which correspond to the intersection of {111} slip planes and the (100) surface, are placed on the free surface. The steps are made infinite through the use of periodic boundary conditions along the $[0\bar{1}1]$ direction. Two steps of opposite signs are introduced in order to allow the use of periodic boundary conditions in the [011] direction normal to the step line. Several calculations on systems with different sizes along [100] and [011] have been performed to evaluate the sample size necessary for the interactions between the surface and the frozen bottom, and between steps to become negligible (Fig. 2). We have varied dimensions from 16 atomic planes up to 120 in both directions. For small boxes, the frozen bottom is too close to the surface which leads to larger elastic limits, for example, it is around −13.7% for the smallest box and it reaches a limit value around −10.0% for larger ones. A typical system encompasses 4 atomic layers along the step line direction $[0\bar{1}1]$, 120 along the surface normal [100] and 160 along [011], i.e., about 80000 atoms. Note that the periodicity of 4 atomic layers along the step direction restricts the problem to two dimensions, and prevents in particular the formation and expansion of such defects as dislocation half-loops.

In this work, the most simple steps formed by the emergence of a perfect dislocation at the surface are considered. They are called D_B rebonded and D_B nonrebonded,[31] and have a height of two atomic layers. The effect of higher steps has also been checked by considering cleavage ledges corresponding to $5D_B$ step forming a {111} facet.

B. Application of a uniaxial stress

To simulate the effect of an applied uniaxial stress $\boldsymbol{\sigma}$, the system is deformed with strains calculated using the silicon compliances S_{ijkl}. These are obtained from the elastic constants C_{ijkl}, computed for all empirical potentials. In this work, the uniaxial stress direction is contained into the surface, but we consider different orientations with respect to the step line. As a result, the projection of this stress in the {111} slip planes, called the resolved shear stress, will also vary. This quantity is important since it is reasonable to assume that the slip system with the largest resolved shear stress along the Burgers vector **b** will be favored. The relationship between the resolved shear stress τ and the uniaxial stress $\boldsymbol{\sigma}$ is $\tau=\pm s|\boldsymbol{\sigma}|$, $s=\cos\varphi\cdot\cos\nu$ being the Schmid factor. φ is the angle between $\boldsymbol{\sigma}$ and the normal of the slip plane and ν the one between $\boldsymbol{\sigma}$ and **b**. In Fig. 3, the calculated Schmid factors along several slip directions into the {111} slip planes are represented as a function of the angle α between the stress orientation and [011], the normal to the step lines (Fig. 2). The most efficient stress orientations for each dislocation (the 60° and screw perfect dislocations, and the 90° and 30° partials) are gathered in Fig. 1(b). The maximum

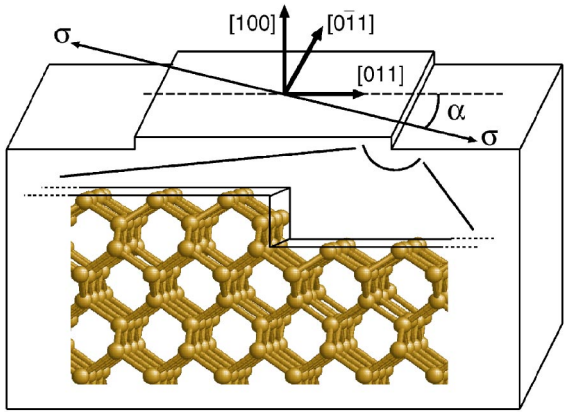

FIG. 2. Calculation cell with a D_B step nonrebonded. $\boldsymbol{\sigma}$ is the applied uniaxial stress and α the angle between the [011] direction (the step normal) and the stress direction. The atomic structure is shown through the enlargement of the step region.

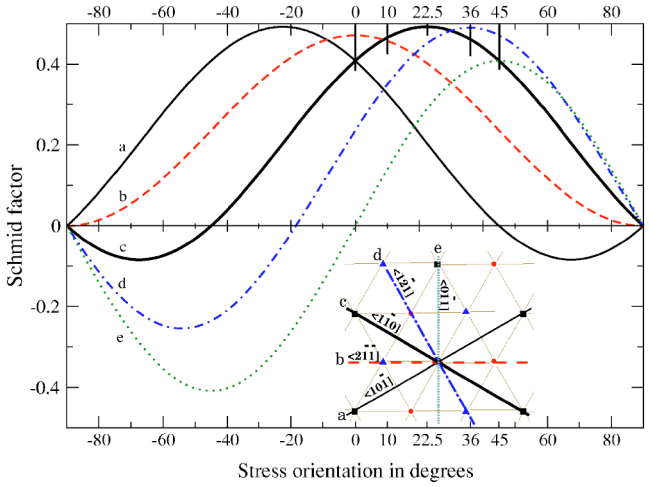

FIG. 3. The Schmid factors versus the stress orientation α are drawn for five slip directions: two along the Burgers vectors of the 60°, $\langle 10\bar{1}\rangle$ (a) and $\langle 1\bar{1}0\rangle$ (c), two along the Burgers vector of the partials, $\langle 2\bar{1}1\rangle$ for the 90° (b) and $\langle 12\bar{1}\rangle$ for the 30° (d) and the last one along $\mathbf{b}_{\text{screw}}$, $\langle 0\bar{1}1\rangle$ (e), parallel to the step line.

resolved shear stress along the Burgers vector of the 60° (screw) is obtained for $\alpha=22.5°$ (45°) for both tensile and compressive stress, respectively. The 90° is favored in case of a nondisorientated tensile stress only ($\alpha=0$). A compressive stress would give a resolved shear stress in the antitwinning sense. Finally, the 30° is favored by a 36° disorientated stress, only in compression, which produces a twinning stress.

C. Computational methods

The large number of atoms required in the simulation prevents the use of *ab initio* methods because it would be too expensive in CPU time. Instead, three classical potentials for silicon are employed: the potential of Stillinger and Weber (SW),[32] based on a linear combination of two- and three-body terms, the Tersoff potential[33] including many-body interactions thanks to a bond order term in the functional form, and the environment-dependent inter-atomic potential[34] (EDIP), more recent and designed specifically for simulating defects.

To deform the system, stress increments of 1.5 GPa (equivalent to a strain around 1 to 1.4% according to the stress orientation) are successively applied, the atomic positions being relaxed between each increment. Two relaxation techniques are used. Either a static relaxation with a conjugate gradients algorithm is performed, until forces on atoms are smaller than 10^{-3} eV/Å, or temperature is introduced in simulations[35] with molecular dynamics, in order to investigate its effect on the nucleation. After an initial static relaxation with conjugate gradients, the temperature is gradually increased with increments of 300 K, the total simulation time ranging from 5 to 50 ps.

III. RESULTS WITH THE STILLINGER-WEBER POTENTIAL

Three temperature domains have been considered; the first one at 0 K, the second one for low temperatures ($\lesssim$900 K) and the last one for high temperatures ($\gtrsim$900 K). In each case, we focused on relevant stress orientations that increase the probability of nucleating the four possible dislocations (60°, screw, 90°, and 30°). Few other stress orientations have also been checked. All results are summarized in Table I. Cases presented concern systems with D_B nonrebonded surface steps. No noticeable changes have been obtained with the D_B rebonded step. The main effect of higher steps, like cleavage ledges, is a slight decrease of the elastic limits. But, the plastic events remain qualitatively similar.

A. Simulations at 0 K

At 0 K, the plastic events appear under large strains in both compression and traction, i.e., greater than 7%

TABLE I. Summary of plastic events obtained with the SW potential, for several stress orientations, at 0 K and with temperature, in traction (positive stress) and in compression (negative stress). Note that the strains along the stress direction are obtained from the linear elasticity theory.

	Elastic limits at 0 K		Results	
α	Stress (GPa)	Strain (%)	$T=0$ K	$T\lesssim 900$ K
0°	31.5	22.9	Fracture	Fracture
	−10.5	−7.6	Micro-twin	Micro-twin
10°	25.5	19.1	Fracture	Perfect 60° then fracture
	−10.5	−7.9	Micro-twin	Micro-twin
22.5°	22.5	18.7	Perfect 60°	Perfect 60°
	−12.0	−10.0	Plastic deformations in {111} planes	Perfect 60°
36°	21.0	19.2	Micro-twins + sometime 60° and screw	Micro-twins + large strained zone
	−13.5	−12.4	Perfect 60°	Perfect 60°
45°	21.0	19.7	Micro-twins	Micro-twins
	−15.0	−14.0	Perfect 60°	Perfect 60°

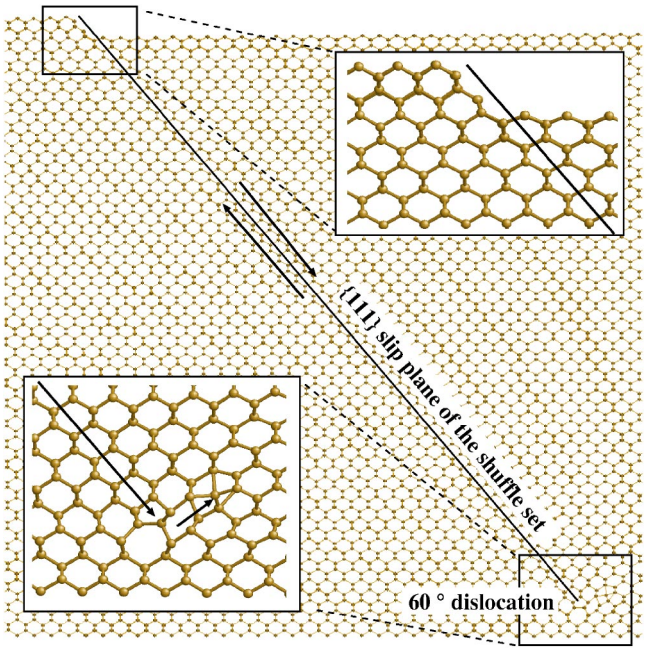

FIG. 4. Nucleation of a perfect 60° dislocation from the surface step in a plane of the shuffle set, with the SW potential. The tensile strain, 22.5° disorientated, is about 18.7%. See the text for details on the insets.

(10.5 GPa) (Table I). They are initiated from the surface, in the close neighborhood of the step. Note that the elastic limits for stressed systems with surface steps are always smaller than for systems without surface steps which have also been calculated. Hence steps facilitate plastic events, by lowering the required stress, and by confining the disturbed surface area. Before the occurrence of plastic events, the system is elastically deformed and the resulting shear strains are mainly located in shuffle set planes.

Investigations have been performed with stress orientations favoring the nucleation of perfect dislocations. For the 60° dislocation, the most efficient angle is $\alpha = 22.5°$ in both traction and compression [Figs. 1(b) and 3]. The results in traction show a relatively large elastic limit of 22.5 GPa (18.7% of strain). Beyond this stress, plasticity occurred (Fig. 4). The inset at the top of the figure clearly shows that the surface step is double after plastic deformation. The displacements in the shuffle set plane crossing the step correspond to the slip of a 60° dislocation. On the second inset into Fig. 4, one can see the dislocation that has stopped at the bottom of the simulation box and another 60° dislocation with the same screw component occurring in the symmetric {111} shuffle set plane from the frozen bottom. Since the dislocation was blocked on the frozen zone (which mimics the bulk) the system found another slip system to continue its relaxation. In compression, large plastic strains appear from the surface steps for a strain of around −10% (−12 GPa), following approximately the {111} planes, but without any clearly identifiable dislocations.

The perfect dislocation in the screw orientation, should be favored by a 45° disorientated stress in both compression and traction [Figs. 1(b) and 3]. However, under a compressive stress, a 60° dislocation instead is nucleated in the shuffle set plane crossing the step. The dislocation decreases the step height and glides in the plane of the shuffle set up to the frozen bottom of the simulation box. Under a tensile stress, defects identified as micro-twins are formed from the surface step. It seems that these defects are due to a peculiar behavior of the SW potential when the resolved shear stress in the {111} planes is along the anti-twinning direction. A previous analysis has shown that these twins are formed by glides in two shuffle set planes with a rotation of trimers in the glide set plane.[36] In brief, in both cases traction and compression, no screw dislocation has been nucleated.

Then, to nucleate partial dislocations, calculations with the most efficient stress orientations have been performed. When a nondisorientated tensile stress favoring the 90° partial is applied on the system [Figs. 1(b) and 3], the relaxation of the atomic positions leads to the crystal fracture. The crack is initiated from the surface step for a stress of 31.5 GPa (22.9%). The best conditions for a 30° partial dislocation are obtained with a 36° disorientated compressive stress. Instead, a perfect 60° dislocation is nucleated in the plane of the shuffle set crossing the surface step. Finally, although the stress orientations are ideal to form partial dislocation according to the Schmid factor, none are nucleated.

We have also checked several other configurations, in particular, nondisorientated compressive stress and 36° disorientated tensile stress favoring anti-twinning configurations. It appeared that in both cases, micro-twins are nucleated from the surface steps, which may be attributed to the somewhat odd behavior of the SW potential described before. In some cases, such as for example a 36° disorientated tensile stress, we obtained complex glide events after deformation. In particular, considering a ledge and not a single step, the structure examination after relaxation revealed the presence of both 60° and screw dislocations. We have also investigated a system under a 10° disorientated tensile stress, for which the resolved shear stresses on the 90° and the 60° dislocations are the same (Fig. 3). This situation gives the same results as a nondisorientated tensile stress, with the fracture of the crystal.

So it seems that at 0 K, in spite of the many stress orientations tested, only perfect dislocations, especially 60°, located in the shuffle set plane passing through the surface step, are nucleated. No dislocations in the glide set planes have been obtained.

B. Other temperatures

The same stress orientations have also been tested in the low temperature domain. The main difference with the 0 K study is the lowering of the elastic limit as the temperature increases, in both traction and compression. For example at 600 K with a 22.5° disorientated stress, it reaches −10.5 GPa in compression and 18 GPa in traction. The results remain qualitatively similar to what has been found at 0 K. Only perfect 60° dislocations are routinely nucleated. And no dislocation has been formed in the glide set plane. Nevertheless, few differences have to be noted. Under a 22.5° disorientated compressive stress favoring the 60° dislocation, the ill-

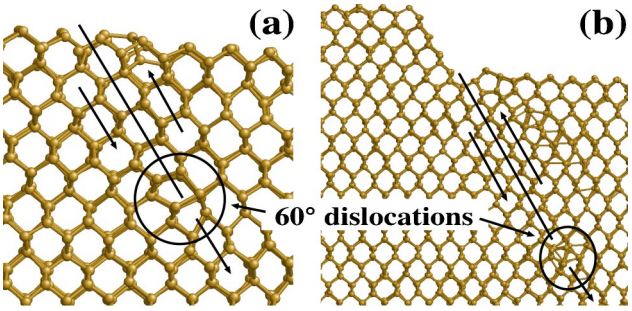

FIG. 5. Nucleation of a perfect 60° dislocation in the shuffle set plane. The compressive stress is 22.5° disorientated. (a) SW: the D_B step disappears for a strain of −7.5% at 900 K; (b) Tersoff: one atomic layer disappears for a strain of −11.0% at 1200 K.

defined plastic strains obtained at 0 K are replaced by a 60° dislocation nucleated in the shuffle set plane [Fig. 5(a)]. In another case, for a 36° disorientated tensile stress leading to a resolved shear stress in the anti-twinning direction, the simultaneous formation of the 60° and screw dislocation at 0 K is replaced by large strained zones near the surface step. These deformations look like a local phase change. The last difference is obtained with a 10° disorientated tensile stress for which the resolved shear stresses on the 90° and 60° dislocations are the same. Our results at low temperature show the nucleation of a 60° dislocation in the shuffle set plane crossing the step. The dislocation glides over a distance of about 15 Å before leading to the fracture of the crystal.

In the high temperature domain, the elastic limits continue to decrease as the temperature is raised. Still, no dislocation in the planes of the glide set is observed. However the stress in the system is now relaxed in a new manner. Previously, at low temperature, the glide events were relatively frequent in the plane of the shuffle set. Now at high temperatures, the glide events in the shuffle set planes become more and more rare as the temperature increases, until they totally disappear. Instead, they are replaced by disorder in the surface along the step line looking like amorphization zones.

IV. RESULTS WITH THE TERSOFF POTENTIAL AND EDIP

The results obtained with the SW potential have shown that only perfect 60° dislocations are nucleated in the shuffle set plane, and at low or zero temperature. A previous study on bulk silicon has shown that the Tersoff potential and EDIP are less reliable than SW in the case of large shear.[37] We have restricted the investigations using these potentials to the 22.5° disorientated tensile or compressive stress favoring the nucleation of a 60° dislocation.

The calculations done with the Tersoff potential at 0 K give very large elastic limits. They are around 46.7% (51 GPa) and −38.5% (−42 GPa) under tensile and compressive stress, respectively. In traction, the crystal periodicity along the step line direction is lost due to large strains of the bulk looking like the beginning of a phase transition [Fig. 6(a)], leading sometimes to a crystal crack from the surface

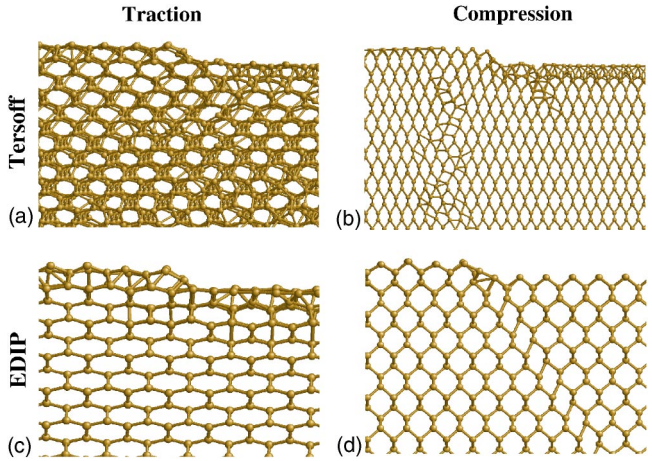

FIG. 6. Snapshot of silicon structures close to the elastic limit with a 22.5° disorientated stress. (a) Tersoff with a strain of 46.7%; (b) Tersoff with a strain of −38.5%; (c) EDIP with a strain of 34.5%; (d) EDIP with a strain of −8.9%.

near the step. In compression, up to −22%, the strains remained homogeneous. Then slight undulations appeared on the surface up to −37%. Finally, a plastic strain occurred in the (011) planes close to the surface step [Fig. 6(b)]. In all cases no glide events are observed. Calculations have been performed at different temperatures and several applied stresses. The only effect is the decrease of the elastic limits and the expansion of plastic strains. However, using high steps (cleavage ledges), a large compressive strain (−11%) and very high temperatures ranging from 1200 K to 1500 K, we managed to nucleate 60° dislocations in the shuffle set plane passing through the step edge [Fig. 5(b)].

The calculations performed with EDIP at 0 K also show much larger elastic limits than the ones obtained with SW. They are around 34.5% (52.5 GPa) in traction and −8.9% (−13.5 GPa) in compression. Under tensile stresses, a crystal crack occurred, while under compressive stresses, the {111} shuffle set plane passing through the step edge is largely sheared [Figs. 6(c) and 6(d)]. This shear propagates from the surface to the slab bottom without dislocation. When the applied strain is increased, neighboring shuffle set planes are also sheared.

V. DISCUSSION

A. Dependency on the potentials

Although the same stress orientations and temperatures have been tried, the results are often different from one potential to another. In order to establish which potential best represents sheared silicon, we have recently compared at 0 K the three potentials with *ab initio* methods based on the density functional theory (DFT) and using the local density approximation (LDA).[37] Here we recall the main conclusions. A homogeneous shear was imposed on {111} planes in a ⟨110⟩ direction, the amplitude of shear going up to 122% for which the diamond cubic structure is recovered. At each shear value, the system was relaxed. When the full amplitude

of the imposed shear has been applied, the crystal structure returned to perfect diamond cubic with the SW potential and EDIP, as well as in the *ab initio* calculation, through a bond breaking and new bond formation across the shuffle plane. However, such a bond switching was not observed with the Tersoff potential which, in these conditions, does not appear suitable for describing dislocation nucleation.

When comparing the bulk silicon energy as a function of the homogeneous shear strain, only the curve of the SW potential is relatively smooth with a shape and amplitude similar to the one calculated in DFT-LDA. The Tersoff curve is discontinuous and the EDIP curve exhibits an angular point. Thus, only SW can account for the atomic surrounding without energy discontinuity when the crystal is largely strained. This feature is even more marked when looking at derivative quantities, related to stresses. In addition, critical quantities such as the theoretical shear strength are overestimated by a factor of about two with the Tersoff potential and EDIP compared to the DFT calculation, whereas Stillinger-Weber is much closer. The SW potential is not fully exempt of drawbacks. When the crystal is sheared in the antitwinning direction,[36] twinning is produced through shearing in the shuffle set planes. But we do not think that this prevents the use of the SW potential for the other stress orientations.

Hopefully, there are indications that these potentials failure may become less important at high temperatures, where dislocations can be formed at lower imposed strains. For example, under a 22.5° disorientated compressive stress, the twin-like defect resulting from the SW potential, is replaced by a 60° dislocation at a smaller strain. Another example is given by the Tersoff potential which at high temperature and for large step height, can lead to the formation of a 60° dislocation. Temperature may rub out unphysical irregularities from the potentials.

Because of its good behavior at 0 K (especially compared to DFT calculations) in the following, only the results obtained with the SW potential will be discussed.

B. Role of the surface step

Here, we focus on the results obtained with the SW potential. Plasticity occurs for very large strains, smaller in compression than in tension. Although the particular crystal structure and potential may be important, one must consider that at the very large stresses considered here, the solid may undergo some buckling instability in compression, instability which helps dislocation formation. A study is in progress to clarify this point.

For bulk silicon, the theoretical strengths obtained with the Stillinger-Weber potential are also large, in agreement with *ab initio* calculations.[38] The presence of a surface decreases the elastic limit, which is decreased again when a step is introduced on the surface. Indeed, the limits of elasticity of the systems with a free surface including steps are definitely smaller than without step. For example at 0 K, for a nondisorientated stress, in tension (compression) the yield strain is about 22.9% (−7.6%) with surface steps and about 28.3% (−11%) without the surface step, respectively. As a rule, the plastic deformations, such as fracture, Glide events or amorphization zones, occur from the steps or in their immediate neighborhood. In fact the presence of the step breaks the symmetry of the system leading to some stress localization near the step. Thus the surface step is a privileged site for the onset of plasticity.

C. Slip system: glide or shuffle

Now, we discuss whether the dislocation nucleation occurs in the glide or in the shuffle set planes, using the results obtained with the SW potential. In principle, the perfect 60° and screw dislocations can be formed in either the glide or the shuffle plane. However from our results, the dislocations are nucleated only in the planes of the shuffle set. The simulations with the stress orientation favoring 90° and 30° partials nucleation in the glide set, lead to the fracture of the crystal and to the formation of a 60° dislocation in the shuffle set, respectively. This result is consistent with the fact that for a slip in the shuffle set, only one covalent bond must be broken compared to three in the glide set.[39]

In the high temperature domain, the probability of dislocation nucleation tends to drop and plastic strains taking the form of amorphizations occur. As temperature is raised, the strain at which plasticity occurs decreases until the thermal vibrations are sufficient to begin the melting/amorphization, but the applied strains are too small to initiate a dislocation in the shuffle set. Still no dislocation is formed in the glide set. Experimentally, at high temperature, the observed dislocations are partial dislocations belonging to the glide set planes. It is commonly accepted that they move more easily through the nucleation and propagation of double kinks.[28,40–42] However, the size of the simulation cell along the dislocation line used here, $4a/2\langle 110\rangle$, is too small to allow the formation of a kink pair. It may explain why only two characterized plastic events are obtained in the simulation: the nucleation of an infinite straight 60° dislocation in the shuffle set planes, or amorphization/melting, depending on the temperature.

In addition, the experimental observations done in both low and high temperature domains reveal a slip mode transition depending on the temperature. At low temperature dislocations seem to glide in the shuffle set planes and at high temperature in the glide set planes.[7,43–45] Whatever the temperature, our simulations have shown that the nucleation of dislocation in the glide set plane is not allowed, because the nucleation of straight dislocation is too expensive in energy and the geometry cell prevents the kink pair nucleation. The only possible dislocations are then nucleated in the shuffle set planes. Moreover we have observed that high temperatures prevent the dislocation formation in this set. Thus our results are not in disagreement with the experimental facts, and complementary calculations in three dimensions are necessary to confirm the slip mode transition.

D. Character of the nucleated dislocation

In order to understand the kind of dislocation formed, we tried to establish the main criteria that govern the nucleation. Usually, when a crystal is stressed, the slip system with the

largest resolved shear stress along the Burgers vector **b** is favored. In our case, the resolved shear stress on each dislocation, proportional to the Schmid factor, is directly related to the stress orientation α. In the range of temperature where the glide events are frequently observed for the SW potential, in most cases, the plastic events are consistent with the predictions from the Schmid factors. For example, in Figs. 1(b) and 3, the 60° dislocation is favored for a 22.5° disorientated stress in both traction and compression, which is obtained in our simulations. Also, a 36° disorientated compressive stress in the twinning sense favors the 30° partial. Since dislocations of the glide set are not activated, as explained above, the system finds another slip system to relax the applied stress. In these twinning conditions, two dislocations are possible: the 60° and the screw. In our simulations, the dislocation nucleated is the 60°, i.e. the one with the largest Schmid factor (Fig. 3).

However several cases cannot be explained on the sole basis of the Schmid factor, the character of the dislocation must also be taken into account. For example, under a nondisorientated tensile stress giving the maximum resolved shear stress along a $\mathbf{b}_{90°}$ partial [Figs. 1(b) and 3], a crystal crack is produced without glide events. Following the Schmid factor analysis, the resolved shear stress is maximum along the [112] direction, i.e., between both 60° dislocations belonging to the shuffle set plane (dislocations in the glide set are not activated). The generalized stacking fault energy calculated along the shuffle set plane in *ab initio*,[46] shows that it is along the [112] direction that the crystal is most resistant to shearing, which explains the crystal cracking. The calculation with a 10° disorientated tensile stress produces a maximum resolved shear stress along a direction slightly disorientated from [112] which allows the 60° dislocation nucleation in agreement with the Schmid factor.

Another interesting case is the 45° disorientated stress [Fig. 3 curves (c) and (e)]. Although the resolved shear stress is the same on the screw and the 60°, the latter is nucleated, in compression. It is worth remarking that the two types of dislocations have different mobility properties, and for instance different Peierls stresses. The calculations performed with the SW potential have shown that the Peierls stress on the 60° dislocation is smaller than on the screw.[47] To relax the applied stress, the nucleation of a perfect 60° dislocation is then favored.

The other discrepancies between the Schmid factor analysis and the simulation results are mainly due to the unphysical defect created by the SW potential, the micro-twins, which appear in both traction and compression when the applied stress acts in the anti-twinning sense. For example in compression at 0 K, the micro-twin formation disappears as the stress orientation angle α increases. Hence in the simulations the resolved shear stress along the anti-twinning direction must be as small as possible to avoid this defect.

Thus, the analysis of the plastic strains as a function of the stress orientation shows that the character of the dislocations nucleated from surface steps can be generally predicted by examining the Schmid factor and the Peierls stress. Another factor may play a role, though, for example, when the maximum resolved shear stress is along the direction where the crystal is most resistant to shearing, leading to fracture.

VI. CONCLUSION

We have investigated the nucleation of dislocations from linear surface defects such as steps, when the system is submitted to a uniaxial stress. Although the elastic limits remain relatively close to the theoretical strength, it appears that the surface steps weaken the atomic structure and help the formation of glide events like dislocations. The glide events are nucleated and propagated in the planes of the shuffle set. No straight dislocation is formed in the glide set plane. The geometry of our simulation cell prevents the formation of kink pairs and does not allow the expected formation of partial dislocations in the glide set at a high temperature. In addition, we have remarked that the high temperature decreases the probability of nucleating a perfect dislocation in the shuffle set plane. The melting/amorphization of silicon occurs before reaching the required shear stress to initiate the dislocation. These results seem consistent with the assumption that at low temperature the dislocations glide in the planes of the shuffle set, based on the observation of nondissociated dislocations in silicon samples deformed at low temperature in conditions preventing failure.[7,45] Additional studies are planned to check the nucleation of dislocation loops in the glide set planes with high temperature.

The role of the stress orientation on the nucleated defects has been studied from the calculations performed with the SW potential. Although the results are slightly biased by the somewhat unphysical defect produced by the SW potential when the stress acts in the anti-twinning direction, it appears that the type of nucleated dislocation could be predicted considering both the resolved shear stress and the Peierls stress.

Finally, although the different results are potential-dependent, only the simulations performed with the SW potential can be taken into account at 0 K as demonstrated in our previous study on a bulk system. It has not been possible to nucleate any dislocations in the simulations performed with the Tersoff potential and EDIP at 0 K. The Tersoff potential has very high energy barriers, preventing the bond breaking required to nucleate a dislocation at low temperatures. The overcoming of the energy barriers leading to dislocation nucleation has become possible at a high temperature. EDIP presents a shear instability in the shuffle set planes at 0 K. By extrapolation, it is probably able to nucleate dislocations thanks to thermal vibrations. We are currently performing *ab initio* simulations of the nucleation of dislocation from surface steps. Although the system is much smaller (about 200 atoms), preliminary results indicate the formation of a 60° dislocation in the shuffle set.

ACKNOWLEDGMENT

Computational facilities at IDRIS (Institut du Développement et des Ressources en Informatique Scientifique) in France have been used for performing some of the calculations.

*Electronic address: julien.godet@etu.univ-poitiers.fr

[1] A. Moulin, M. Condat, and L. P. Kubin, Philos. Mag. A **79**, 1995 (1999).
[2] J. Dunstan, J. Mater. Sci.: Mater. Electron. **8**, 337 (1997).
[3] S. C. Jain, A. H. Harker, and R. A. Cowley, Philos. Mag. A **75**, 1461 (1997).
[4] R. X. Wu and G. C. Weatherly, Philos. Mag. A **81**, 1489 (2001).
[5] Y. Q. Wu and Y. B. Xu, Philos. Mag. Lett. **78**, 9 (1998).
[6] C. Scandian, H. Azzouzi, N. Maloufi, G. Michot, and A. George, Phys. Status Solidi A **171**, 67 (1999).
[7] J. Rabier, P. Cordier, J. L. Demenet, and H. Garem, Mater. Sci. Eng., A **A309-A310**, 74 (2001).
[8] P. Pirouz, J. L. Demenet, and M. H. Hong, Philos. Mag. A **81**, 1207 (2001).
[9] P. Pirouz, A. V. Samant, M. H. Hong, A. Moulin, and L. P. Kubin, J. Mater. Res. **14**, 2783 (1999).
[10] F. C. Frank, in *Symposium on Plastic Deformation of Crystalline Solids* (Carnegie Institute of Technology, Pittsburgh, 1950), p. 89.
[11] S. V. Kamat and J. P. Hirth, J. Appl. Phys. **67**, 6844 (1990).
[12] G. E. Beltz and L. B. Freund, Phys. Status Solidi B **180**, 303 (1993).
[13] G. E. Beltz and L. B. Freund, in *Thin-Films: Stresses and Mechanical Properties V. Symposium*, edited by S. P. Baker, C. A. Ross, P. H. Townsend, C. A. Volkert, and P. Borgesen, (Materials Research Society, Pittsburgh, 1995), p. 93.
[14] M. Ichimura and J. Narayan, Mater. Sci. Eng., B **31**, 299 (1995).
[15] A. Aslanides and V. Pontikis, Philos. Mag. Lett. **78**, 377 (1998).
[16] Y.-M. Juan, Y. Sun, and E. Kaxiras, Philos. Mag. Lett. **73**, 233 (1996).
[17] H. Gao, C. S. Ozkan, W. D. Nix, J. A. Zimmerman, and L. B. Freund, Philos. Mag. A **79**, 349 (1999).
[18] G. Xu, A. S. Argon, and M. Ortiz, Philos. Mag. A **75**, 341 (1997).
[19] A. George and G. Michot, Mater. Sci. Eng., A **164**, 118 (1993).
[20] G. Michot, H. Azzouzi, N. Maloufi, M. L. de Oliviera, C. Scandia, and A. George, in *Multiscale Phenomena in Plasticity*, edited by J. Lépinoux, D. Mazière, V. Pontikis, and G. Saada (Kluwer Academic, Dordrecht, 1999), Vol. 367 of NATO ASI Series E: Applied Sciences, p. 117.
[21] B. J. Gally and A. S. Argon, Philos. Mag. A **81**, 699 (2001).
[22] A. S. Argon and B. J. Gally, Scr. Mater. **45**, 1287 (2001).
[23] X. J. Ning and N. Huvey, Philos. Mag. Lett. **74**, 241 (1996).
[24] S. Brochard, P. Beauchamp, and J. Grilhé, Philos. Mag. A **80**, 503 (2000).
[25] S. Brochard, P. Beauchamp, and J. Grilhé, Phys. Rev. B **61**, 8707 (2000).
[26] T. W. Poon, S. Yip, P. S. Ho, and F. F. Abraham, Phys. Rev. B **45**, 3521 (1992).
[27] J. Godet, L. Pizzagalli, S. Brochard, and P. Beauchamp, Scr. Mater. **47**, 481 (2002).
[28] J. P. Hirth and J. Lothe, *Theory of Dislocations*, 2nd ed. (Wiley, New York, 1982).
[29] D. J. Chadi, Phys. Rev. Lett. **43**, 43 (1979).
[30] A. Ramstad, G. Brocks, and P. J. Kelly, Phys. Rev. B **51**, 14 504 (1995).
[31] D. J. Chadi, Phys. Rev. Lett. **59**, 1691 (1987).
[32] F. H. Stillinger and T. A. Weber, Phys. Rev. B **31**, 5262 (1985).
[33] J. Tersoff, Phys. Rev. B **39**, 5566 (1989).
[34] M. Z. Bazant, E. Kaxiras, and J. F. Justo, Phys. Rev. B **56**, 8542 (1997).
[35] J. Rifkin, *Xmd—Molecular Dynamics Program*, www.ims.uconn.edu/centers/simul/♯software (1999), jon.rifkin@uconn.edu
[36] J. Godet, L. Pizzagalli, S. Brochard, and P. Beauchamp, Comput. Mater. Sci. **30**, 16 (2004).
[37] J. Godet, L. Pizzagalli, S. Brochard, and P. Beauchamp, J. Phys.: Condens. Matter **15**, 6943 (2003).
[38] D. Roundy and M. L. Cohen, Phys. Rev. B **64**, 212103 (2001).
[39] W. Shockley, Phys. Rev. **91**, 1563 (1953).
[40] V. V. Bulatov, S. Yip, and A. S. Argon, Philos. Mag. A **72**, 453 (1995).
[41] V. V. Bulatov, J. F. Justo, W. Cai, S. Yip, A. S. Argon, T. Lenosky, M. de Koning, and T. D. de la Rubia, Philos. Mag. A **81**, 1257 (2001).
[42] T. E. Mitchell, P. M. Anderson, M. I. Baskes, S. P. Chen, R. G. Hoagland, and A. Misra, Philos. Mag. **83**, 1329 (2003).
[43] M. S. Duesbery and B. Joós, Philos. Mag. Lett. **74**, 253 (1996).
[44] J. Rabier, P. Cordier, T. Tondellier, J. L. Demenet, and H. Garem, J. Phys.: Condens. Matter **12**, 10059 (2000).
[45] J. Rabier and J. L. Demenet, Scr. Mater. **45**, 1259 (2001).
[46] Y.-M. Juan and E. Kaxiras, Philos. Mag. A **74**, 1367 (1996).
[47] Q. Ren, B. Joos, and M. S. Duesbery, Phys. Rev. B **52**, 13 223 (1995).